Cancer Immunol Immunother (2010) 59:675–686
DOI 10.1007/s00262-009-0783-7

ORIGINAL ARTICLE

Nuclear factor kappaB-activated monocytes contribute to pancreatic cancer progression through the production of Shh

Akio Yamasaki · Chizu Kameda · Rui Xu · Haruo Tanaka · Takehiko Tasaka · Nobuhito Chikazawa · Hiroyuki Suzuki · Takashi Morisaki · Makoto Kubo · Hideya Onishi · Masao Tanaka · Mitsuo Katano

Received: 26 June 2009 / Accepted: 9 October 2009 / Published online: 28 October 2009

Abstract Recently, it was reported that Hh signaling is activated in tumor stromal cells but not in tumor cells themselves and that stromal cells may play a role in the proliferation of cancer cells. This suggests the possibility that stromal cells have an important role in the proliferation of tumor cells that may be mediated through Hh signaling. In this report, we present for the first time that inflammation-stimulated monocytes produce Shh through activation of the NF-κB signaling pathway, and that the Shh produced promotes the proliferation of pancreatic cancer cells in a paracrine manner through Hh signaling.

Keywords NF-κB · Hh pathway · Monocytes · Pancreatic cancer

Abbreviations

PBMCs	Peripheral blood mononuclear cells
Shh	Sonic hedgehog
PDAC	Pancreatic ductal adenocarcinomas

A. Yamasaki · C. Kameda · R. Xu · H. Tanaka · T. Tasaka · N. Chikazawa · H. Suzuki · T. Morisaki · H. Onishi · M. Katano (✉)
Department of Cancer Therapy and Research, Graduate School of Medical Sciences, Kyushu University, 3-1-1 Maidashi, Higashi-ku, Fukuoka 812-8582, Japan
e-mail: mkatano@tumor.med.kyushu-u.ac.jp

A. Yamasaki
e-mail: y-akio@surg1.med.kyushu-u.ac.jp

M. Kubo · M. Tanaka
Department of Surgery and Oncology, Graduate School of Medical Sciences, Kyushu University, Fukuoka, Japan

Introduction

Pancreatic cancer is one of the most lethal of malignancies. Therapeutic options for patients with unresectable, metastatic, recurrent diseases are extremely limited, and the 5-year survival rate is below 5%. Thus, new therapeutic options are required.

Recent studies have proposed that the hedgehog (Hh) signaling pathway, a morphogenesis signaling pathway, contributes to pancreatic carcinogenesis. It has been shown for the first time that the expression of a Hh ligand, Sonic hedgehog (Shh), and essential components of the pathways, including patched (Ptch) and smoothed (Smo), have been found in up to 70% of human pancreatic ductal adenocarcinomas (PDAC) specimens [35] and may have an early and critical role in the genesis of PDAC [3, 35]. In these reports, it has also been shown that Shh overexpression is sufficient to initiate PanIN (pancreatic intraepithelial neoplasia)-like precursor lesions. Furthermore, it has been shown that Shh overexpression accelerates tumor formation in mouse orthotopic xenotransplants [23]. These studies have strongly suggested that Shh produced by tumor cells activates the Hh pathway and tumor cell growth in an autocrine/juxtacrine manner [27, 35]. Based on these observations, Hh pathway inhibitors are now under development as a new therapeutic option for PDAC. Quite recently, however, Yauch et al. [38] demonstrated that ligand-dependent activation of the Hh pathway was found in the stromal microenvironment, but not in tumor epithelial cells, in a xenograft tumor model and that the specific inhibition of Hh signaling in the mouse stroma results in growth inhibition. If so, their data indicate a paracrine requirement for Hh ligand signaling in pancreatic carcinogenesis. They propose that Hh ligands produced by tumor cells act on the stromal compartment to support tumor growth indirectly.

Thus, the mechanisms by which the Hh pathway, especially Shh, contributes to pancreatic carcinogenesis remains unclear and controversial.

As we know, epidemiological studies have long indicated a strong association between chronic inflammation and the initiation and progression of PDAC. For example, smoking, *Helicobacter pylori* seropositivity, and chronic pancreatitis are considered risk factors for PDAC [2, 4, 21, 26, 30]. However, molecular mechanisms linking inflammation and the development of epithelial cancer have remained unclear. Recently, the significance of nuclear factor kappaB (NF-κB) was proposed [9, 16, 22]. NF-κB is a transcription factor that controls expression of numerous genes involved in inflammation [15]. In fact, it has been suspected that NF-κB signaling has a pivotal role in chronic inflammation-associated malignancies. Recent data suggest that NF-κB activation in tumor stromal cells contributes to tumorigenesis by upregulating tumor-promoting proinflammatory proteins including angiogenic factors, matrix metalloproteases and reactive oxygen and nitrogen species, which increase DNA damage [20, 29].

Importantly, we have indicated a close linkage between NF-κB and Shh expression in PDAC cells [25], and thereafter it was shown that Shh is a direct transcriptional target of NF-κB [17]. These findings suggest that the NF-κB–Shh pathway may play an important role in the linkage between inflammation and the carcinogenesis of PDAC. By linking each of these findings, we hypothesized that monocytes activated with inflammatory stimuli such as lipopolysaccharide (LPS) may play an important role, directly or indirectly, through Shh production in the initiation and progression of PDAC.

Materials and methods

Cell culture, reagents, and antibodies

Peripheral blood mononuclear cells (PBMCs) were isolated from heparinized peripheral blood by HISTOPAQUE-1077 (Sigma–Aldrich, St. Louis, MO, USA) density gradient centrifugation. PBMCs were resuspended in RPMI 1640 basal medium (Nacalai Tesque, Kyoto, Japan) supplemented with 1% human albumin (Mitsubishi Tanabe Pharma, Osaka, Japan) 100 units/mL penicillin (Meiji Seika, Tokyo, Japan) and 100 μg/mL streptomycin (Meiji Seika), plated at a density of 8×10^6 cells/ml, and allowed to adhere for 30 min at 37°C in six-well plates (Nalge Nunc International, Chiba, Japan). Non-adherent cells and adherent cells were collected separately. After collecting these cells, adherent and non-adherent cells were incubated for 1 h with fluorescently conjugated CD14 and CD2 antibodies (BD Pharmingen, San Diego, CA, USA), respectively. The fluorescently labeled cells were applied to a FACSCalibur flow cytometer (Becton–Dickinson, Franklin Lakes, NJ, USA) and the fluorescence intensity was analyzed using CELLQuest software (Becton–Dickinson). The procedure of plastic adherence was repeated until CD14 and CD2 positive cells constituted over 90% of adherent and non-adherent cells, respectively. Purified cells were resuspended in RPMI 1640 basal medium supplemented with 1% human albumin.

Two human PDAC cell lines (AsPC-1 and SUIT-2) and a human acute monocytic leukemia cell line, THP-1, were maintained in complete medium consisting of RPMI 1640 supplemented with 10% fetal bovine serum (FBS: Biological Industries, Kibbutz Beit Haemek, Israel), 100 units/mL penicillin (Meiji Seika) and 100 μg/mL streptomycin (Meiji Seika) at 37°C.

LPS from *Escherichia coli* (B4) and NF-κB inhibitor, pyrrolidine dithiocarbamate (PDTC) were purchased from Sigma (Deisenhofen, Germany) and recombinant human Shh N-terminal peptide (rhShh) was purchased from R&D Systems (Minneapolis, MN, USA). Cyclopamine, purchased from Toronto Research Chemicals (Toronto, Canada), was diluted in 100% methanol.

Rabbit anti-Shh (sc-9024) antibody was purchased from Santa Cruz Biotechnology (Santa Cruz, CA, USA). Mouse anti-CD68 (PG-M1) antibody was from Dako (Grostrup, Denmark). Mouse anti-Shh blocking antibody (5E1), developed by Thomas M. Jessell, was obtained from the Developmental Studies Hybridoma Bank developed under the auspices of the National Institute of Child Health and Human Development and maintained by The University of Iowa, Department of Biological Sciences (Iowa City, IA). Control mouse IgG was purchased from Sigma–Aldrich (St Louis, MO).

Clinical samples and fluorescence immunohistochemistry

Surgical specimens were obtained from 20 patients with PDAC, all of whom underwent resection at the Department of Surgery and Oncology, Kyushu University (Fukuoka, Japan). Informed consent was obtained from all patients. Samples were fixed in 10% formalin and embedded in paraffin. Slides were dewaxed, rehydrated, washed, and subjected to microwave retrieval in a citrate buffer (pH 6.0). For immunofluorescence double staining, sections were double-stained with rabbit anti-Shh (sc-9024; 1:100) and mouse monoclonal anti-CD68 (clone PG-M1; 1:100). The bound antibodies were visualized using goat anti-rabbit IgG (H + L) Alexa 488 (Invitrogen, Carlsbad, CA, USA) and goat anti-mouse (H + L) Alexa 568 (Invitrogen). The stained sections were photographed with a digital camera attached to a Zeiss Axio Imager A1 microscope (Carl Zeiss, Oberknochen, Germany).

Fluorescence immunocytochemistry

Cells were seeded onto pre-underlaid poly L-lysine-coated glass coverslips (Asahi Techno Glass, Chiba, Japan) in 24-well plates, and were incubated overnight in RPMI containing 10% FBS. Twenty-four-well plates were centrifuged for adherence, and then cells were fixed in 4% paraformaldehyde followed by permeabilization with 0.2% Triton X-100, before overnight incubation at 4°C with rabbit anti-Shh primary antibody (1:200, Santa Cruz) followed by an appropriate secondary antibody, goat anti-rabbit IgG (Invitrogen). Cells were counterstained with 4′,6′-diamidino-2-phenylindole dihydrochloride (Sigma–Aldrich). After mounting in Vectashield (Vector Laboratories), samples were examined by fluorescence microscopy (Carl Zeiss).

Real-time reverse transcription-PCR

RNA (1 μg) was treated with DNase and reverse transcribed to cDNA with the Quantitect Reverse Transcription kit (Qiagen, Valencia, CA, USA) according to the manufacturer's protocol. Reactions were run with the iQ SYBR Green Supermix (Bio-Rad, Hercules, CA, USA) on a DNA Engine Opticon 2 System (MJ Research, Waltham, MA). The amount of each target gene in a given sample was normalized to the level of β-actin in that sample. Each sample was run in triplicate. All primer sets amplified fragments <200 bp long. Sequences of the primers used were *β-actin* forward, 5′-TTGCCGACAGGATGCAGAAGGA-3′, and reverse, 5′-AGGTGGACAGCGAGGCCAGGAT-3′; *Shh* forward, 5′-GTGTACTACGAGTCCAAGGCAC-3′, and reverse, 5′-AGGAAGTCGCTGTAGAGCAGC-3′; *Smo* forward, 5′-CAGGTGGATGGGGACTCTGTGAGT-3′, and reverse, 5′-GAGTCATGACTCCTCGGATGAGG-3′; *Gli1* forward, 5′-ATTGCCAGTCATTTCCACACCA-3′, and reverse, 5′-CTCGGGCACCATCCATTTCTAC-3′.

Luciferase assay

Cells in six-well plates were transfected with plasmids with SuperFect transfection reagent (Qiagen) according to the manufacturer's instructions. Cells on each well were co-transfected with 5 ng pRLSV40 (Promega) and 2 μg pELAM-Luc [27], the NF-κB-dependent luciferase reporter was kindly provided by Dr. K. Takeda, from the Division of Embryonic and Genetic Engineering, Medical Institute of Bioregulation, Kyushu University. LPS was added to each well and luciferase assays were performed 6 h later with the dual luciferase assay kit (Promega) according to the manufacturer's instructions. The luciferase activities were normalized to the *Renilla* luciferase activity.

Electrophoretic mobility shift assay (EMSA)

Preparation of nuclear extracts from THP1 cells and PBMCs were performed as described previously [37]. Briefly, 3×10^6 cells cocultured with LPS for the indicated times were collected and washed once with PBS. THP1 cells were then homogenized in hypotonic buffer [10 mM HEPES (pH 7.5), 10 mM KCl, 1.5 mM $MgCl_2$, 0.1% NP40, and 5% protease inhibitor mixture]. Nuclear extract (10 μg) was then incubated for 30 min at 37°C with binding buffer [60 mmol/L HEPES (pH 7.5), 180 mmol/L KCl, 15 mmol/L $MgCl_2$, 0.6 mmol/L EDTA, 24% glycerol], poly (deoxyinosinic-deoxycytidylic acid), and [32] P-labeled double-stranded oligonucleotides containing the NF-κB and Oct-1 binding motif (Promega, Madison, WI, USA). Sequences of the double-stranded oligomer used for the EMSA were 5′-AGTTGAGGGGACTTTCCCAG GC-3′ for NF-κB and 5′-TGTCGAATGCAAATCACTA GAA-3′ for Oct-1. The reaction mixtures were loaded onto a 4% polyacrylamide gel and electrophoresed with a running buffer of 0.25% Tris-borate EDTA. Gels were dried and the DNA–protein complexes were visualized by autoradiography.

Proliferation assay

Cells (2×10^4 per well) seeded in 12-well plates in complete culture medium were incubated overnight. Medium was changed to RPMI 1640 with 1% FBS in the presence or the absence of rhShh N-terminal peptide, mouse anti-Shh blocking antibody (5E1), control mouse IgG antibody, and cyclopamine (Toronto Research Chemicals). After 3 days of incubation, cells were counted with a Coulter counter (Beckman Coulter, Fullerton, CA, USA).

In our coculture system, cell proliferation was analyzed by Coulter counter cell analysis and FACS analysis as previously reported [18]. In brief, PDAC cells (1×10^5 cells per well) were labeled with 5 μM CFSE by using the CellTrace™ CFSE Cell Proliferation kit (Invitrogen) prior to coculture with THP-1 cells (1×10^5 cells per well). THP-1 cells were cultured in the presence or absence of LPS for 24 h. THP-1 cells were then washed intensively to eliminate LPS and the cell number was readjusted. Each of LPS-stimulated and non-stimulated THP-1 cells were then mixed with CFSE-labeled pancreatic cancer cells and cultured for a further 4 days. After 4 days of incubation, the cells were harvested by trypsinization and total cell number was counted with a Coulter counter. The fractions of THP-1 cells and PDAC cells were determined using a FACSCalibur™ (Becton–Dickinson) and the absolute number of PDAC cells was calculated.

Semiquantitative RT-PCR

Total RNA was extracted from PBMCs and adherent cells using the guanidinium thiocyanate–phenol–chloroform single-step method [7] and quantified by spectrophotometry (Ultrospec 2100 Pro; Amersham Pharmacia Biotech, Cambridge, United Kingdom). *Shh* forward, 5′-CGCACG GGGACAGCTCGGAAGT-3′ and reverse, 5′-CTGCGCG GCCCTCGTAGTGC-3′ primers yield a 492-bp product. *Gli1* forward, 5′-TCTGCCCCCATTGCCCACTTG-3′ and reverse, 5′-TACATAGCCCCCAGCCCATACCTC-3′ primers yield a 480-bp product. *Ptch1* forward, 5′-CGGCGTTC TCAATGGGCTGGTTTT-3′ and reverse, 5′-GTGGGGCT GCTGTCTCGGGTTCG-3′ primers yield a 376-bp product. *β-actin* forward, 5′-TTGTTACAGGAAGTCCCTTGCC3′ and reverse, 5′-ATGCTATCACCTCCCCTGTGTG-3′ primers gave rise to a 436-bp product. Amplification conditions comprised an initial denaturation for 2 min at 94°C followed by 30 cycles of 1 min at 94°C, 1 min at 58°C, and 1 min at 72°C. Amplification of each gene was in the linear range. The PCR products were separated on ethidium bromide-stained 2% agarose gels.

Immunoblotting

Whole-cell extraction was carried out with M-PER Reagents (Pierce Biotechnology, Rockford, IL) according to the manufacturer's instructions. Protein concentrations were determined with a Bio-Rad Protein Assay (Bio-Rad). Whole-cell extract (50 μg) was separated by electrophoresis on 12.5% SDS-polyacrylamide gels and transferred to Protran nitrocellulose membranes (Schleicher and Schnell BioScience, Dassel, Germany). Blots were incubated with anti-Shh pAb (1:100, Santa Cruz) or anti-α-tubulin mAb (1:1,000, Sigma–Aldrich) overnight at 4°C. Blots were then incubated with secondary antibody, horseradish peroxidase-linked anti-rabbit IgG antibody (Amersham Biosciences, Piscataway, NJ) at room temperature for 1 h. Immunocomplexes were detected with an enhanced chemiluminescence reagent (Amersham Biosciences) and visualized with a Molecular Imager FX (Bio-Rad).

Plasmids, oligodeoxynucleotides, and cell transduction

Phosphorothioated and double-stranded NF-κB decoy oligodeoxynucleotides, 5′-CCTTGAAGGGATTTCCCTCC-3′, and scramble oligodeoxynucleotides, 5′-TTGCCGTACCT GACTTAGCC-3′, were purchased from Hokkaido System Science (Sapporo, Japan). Cells were transfected with 0.5 μmol/L NF-κB decoy or scramble oligodeoxynucleotides with LipofectAMINE (Life Technologies, Inc, Gaithersburg, MD) according to the manufacturer's instructions. Transfected cells were used for experiments 48 h after transfection. The pIRES2-hSHH-EGFP (referred to as pSHH-GFP) plasmids were kindly provided by Dr. Aubie Shaw (Division of Urology, Department of Surgery, University of Wisconsin, Madison, WI; [11]). The pCMV-IκBα wild type (WT) and pCMV-IκBα mutant were purchased from BD Biosciences/Clontech (Palo Alto, CA). Cells seeded in six-well plates were transfected with 2 μg plasmid with TransFast reagent (Promega, Madison, WI) according to the manufacturer's protocol.

RNA interference

The siRNA for *Shh* (ON-TARGET*plus* SMART pool, L-006036), *Smo* (ON-TARGET*plus* SMART pool, L-005726) and negative control siRNA (ONTARGET*plus* siCONTROL non-targeting pool, D-001810) were purchased from Dharmacon RNA Technologies (Chicago, IL, USA). Cells seeded in six-well plates were transfected with 100 nM siRNA using Lipofectamine RNAiMAX Reagent (Invitrogen) according to the manufacturer's instructions. Cells were used for experiments at the indicated times after transfection.

Statistical analysis

Mann–Whitney's *U* tests were used for statistical analysis. All results with a P value of <0.05 were considered statistically significant.

Results

LPS increases Shh expression and a NF-κB inhibitor PDTC suppresses the increased Shh expression in human peripheral blood monocytes.

Since our previous study indicated a possible linkage between Shh expression and NF-κB activation in PDAC [25], we first examined if a well-known NF-κB activator, LPS, could induce increased expression of Shh in PBMCs. As expected, LPS increased the expression of Shh at the mRNA level in a time- and dose-dependent manner (Fig. 1a, b). LPS at 10 μg/ml also clearly increased Shh expression in PBMCs at the protein level (Fig. 1c). The Shh protein level was quantified with the 19-kDa fragment because it is the physiologic form of Shh [5, 19]. Next, we examined which subpopulations in PBMCs increased Shh expression on LPS stimulation. As described in the "Materials and methods" section, we separately collected plastic non-adherent and adherent cells from PBMCs. Thereafter, these cells were analyzed by flow cytometry. When CD2 or CD14-positive cells were over 90%, they were used as non-adherent or adherent cells, respectively. LPS significantly increased Shh expression in adherent

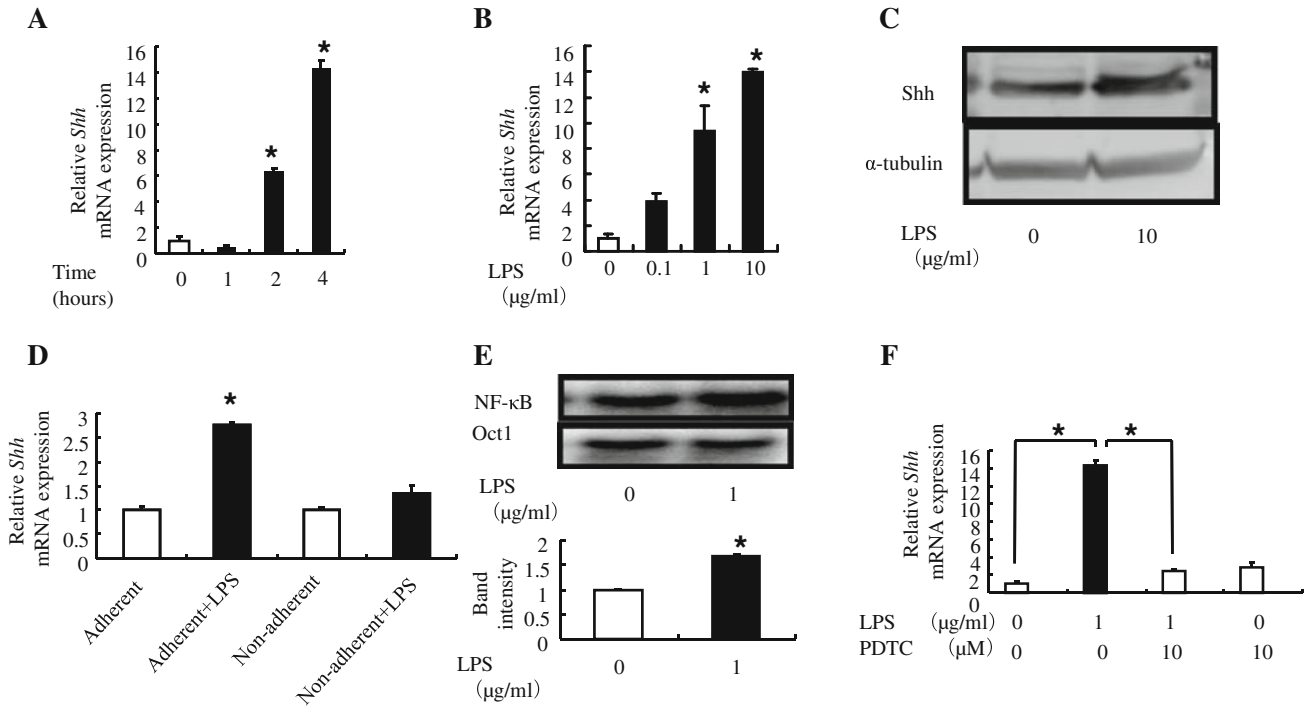

Fig. 1 LPS can induce Shh expression in human monocytes and a NF-κB inhibitor PDTC can suppress the increased Shh expression. **a** PBMCs were treated with 10 μg/ml LPS for the indicated times and *Shh* mRNA expression was examined by real-time PCR. **b** PBMCs were treated with LPS at the indicated concentrations for 4 h and *Shh* mRNA was evaluated by real-time PCR. **c** Shh protein expression in PBMCs treated with 10 μg/ml LPS was evaluated by Western Blot. 50 μg of protein was used. α-tubulin was used as loading control. **d** Plastic non-adherent and adherent cells from PBMCs were separately collected. Non-adherent cells and adherent cells were treated with or without 1 μg/ml LPS for 4 h and then *Shh* mRNA in these cells were evaluated by real-time PCR. **e** Increased NF-κB activation in adherent cells. NF-κB activation in adherent cells treated with 1 μg/ml LPS was evaluated by EMSA. Oct1 was used as loading control. The *lower panel* shows normalized NF-κB expression. **f** Adherent cells were treated with 10 μM PDTC for 24 h, and were cultured with or without 1 μg/ml LPS for additional 12 h. Then *Shh* mRNA expression was estimated by real-time PCR. *Bars* SD. $*P < 0.05$

cells compared with that in non-adherent cells, indicating that the main source of Shh expression induced with LPS is CD14-positive monocytes (Fig. 1d). To investigate the contribution of the NF-κB pathway to LPS-induced Shh expression in monocytes, we examined if NF-κB inhibition can inhibit Shh expression induced by LPS by EMSA. LPS induced an increase in NF-κB p65 DNA binding activity in monocytes, indicating increased NF-κB activation by LPS (Fig. 1e). As we expected, LPS-induced *Shh* mRNA expression was almost completely suppressed by the NF-κB inhibitor PDTC (Fig. 1f). These data indicate that increased NF-κB activation contributes to the increased Shh expression induced by LPS.

LPS increases Shh expression in THP-1 cells and blockade of NF-κB activation suppresses LPS-induced Shh expression.

The individual variation of biological functions of human monocytes is large and it is not necessarily easy to obtain the number of cells required for experiments. And, primary monocytes do not proliferate on a suitable scale so that their use for functional studies in vitro is limited. Many in vitro studies therefore use immortalized proliferative cell lines instead of primary monocytes. Especially, THP-1 cell line is a well-established and widely used model for investigating the biological function of human monocytes and macrophages [1, 6, 8, 14, 28, 33, 39]. Therefore, to study the molecular mechanisms of the biological functions of monocyte-secreted Shh, we used THP-1 cells, instead of human monocytes. LPS increased *Shh* mRNA expression in THP-1 cells in a time- and dose-dependent manner (Fig. 2a, b). Increased expression of Shh by LPS was shown at the protein level by immunofluorescence, too (Fig. 2c). Western blot analysis also showed increased expression of Shh by LPS (Fig. 2d). Like monocytes, LPS increased NF-κB p65 DNA binding activity in THP-1 cells in a time- and dose-dependent manner (Fig. 3a, b). NF-κB activation by LPS was also confirmed using a NF-κB reporter assay. LPS increased transcriptional activity of NF-κB in a time- and dose-dependent manner (Fig. 3c, d). Next, to clarify the linkage between LPS-induced NF-κB activation and LPS-induced Shh expression, we used three NF-κB inhibitors which act at different points in the NF-κB pathway. Although inhibitory activity of PDTC is relatively specific to NF-κB, detailed mechanisms are still unknown [34].

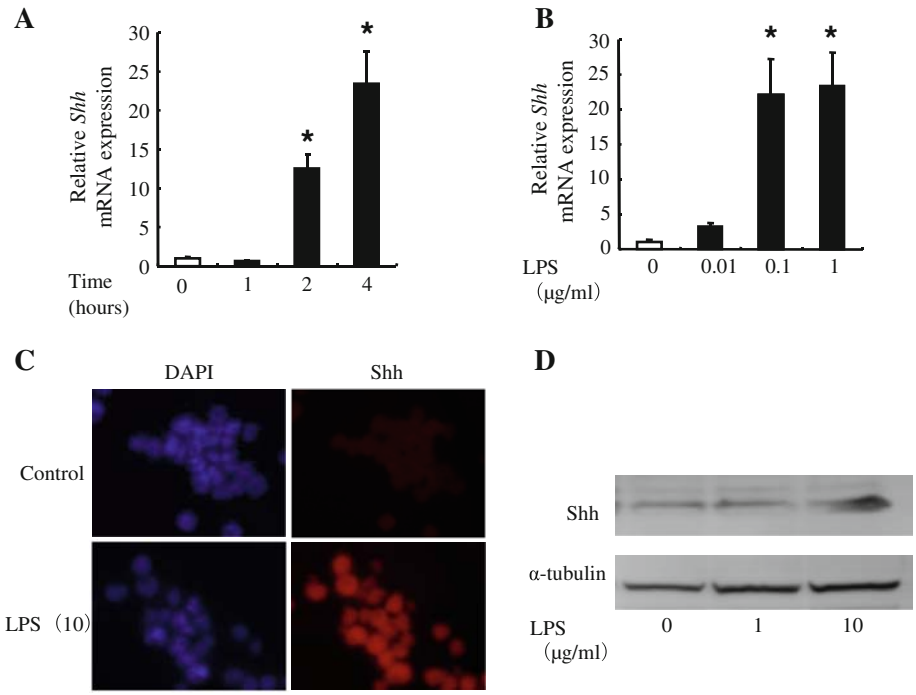

Fig. 2 LPS can induce Shh expression in THP-1 cells at mRNA and protein levels. **a** THP-1 cells were treated with 1 μg/ml LPS for the indicated times and *Shh* mRNA expression was examined by real-time PCR. **b** THP-1 cells were treated with LPS at the indicated concentrations for 4 h, and *Shh* mRNA level was examined by real-time PCR. **c** Representative pictures of immunocytochemistry. THP-1 cells were treated with 10 μg/ml LPS for 24 h. Then Shh protein expressions were evaluated. DAPI was used for nuclear staining. **d** Western blot analysis. THP-1 cells were treated with LPS at the indicated concentrations for 24 h. Then 50 μg of cell lysate was blotted. α-tubulin was used as loading control. *Bars* SD. *$P < 0.05$

IκBα mutant and NF-κB decoy inhibit phosphorylation of NF-κB and DNA binding of NF-κB, respectively. All three inhibitors (PDTC, IκBα mutant and NF-κB decoy) almost completely suppressed LPS-induced *Shh* mRNA expression (Fig. 3e).

Shh produced by LPS-stimulated THP-1 cells promotes proliferation of pancreatic cancer cells

We examined whether Shh produced by LPS-stimulated THP-1 cells could promote the proliferation of pancreatic cancer cells. In the present study, we used two human pancreatic cell lines, AsPC-1 and SUIT-2 cells, because detailed information concerning the Hh pathway has already been obtained from our previous studies [24, 25]. Briefly, both cells express Hh pathway-related molecules including *Shh, Ptch1* and *Gli1* at the mRNA levels and the Hh pathway is constitutively activated as indicated by *Gli1* mRNA expression (Fig. 4a). When recombinant Shh (rh Shh) was added, *Gli1* m RNA expression significantly increased. In contrast, when anti-Shh blocking antibody (5E1) was added, *Gli1* mRNA expression significantly suppressed (Fig. 4b). Recombinant human Shh peptide increases proliferation of these cells and anti-Shh blocking antibody (5E1) decreases proliferation of these cells (Fig. 4c). A Hh pathway inhibitor, cyclopamine also decreases proliferation of these cells (Fig. 4d). These findings strongly indicate a ligand-dependent activation of the Hh pathway in these cells and a contribution of the Hh pathway to the proliferation of these cells. When these cells were cocultured with THP-1 cells, LPS-stimulated THP-1 cells significantly enhanced proliferation of these cells compared with non-stimulated THP-1 cells (Fig. 5a). LPS-stimulated THP-1 cell-dependent increased proliferation was suppressed by the Shh antibody, 5E1 (Fig. 5a). As shown in Fig. 4, these cells produce Shh and proliferate in an autocrine manner. To clarify the contribution of THP-1 cell-produced Shh to increased proliferation of pancreatic cancer cells, we silenced *Shh* mRNA expression in these cancer cells using small interfering RNA (Fig. 5b, left panels). As expected, the proliferation of Shh-silenced cancer cells significantly decreased compared with that of wild-type cancer cells (data not shown). LPS-stimulated THP-1 cells also enhanced the proliferation of Shh-silenced cancer cells, compared with non-stimulated THP-1 cells, an action that was significantly suppressed by 5E1 (Fig. 5b, right panels). These findings indicate that Shh produced by LPS-stimulated THP-1 cells play an important role in proliferation of these PDAC cells in a paracrine manner. To further clarify that LPS-stimulated THP-1 cell producing Shh increases the proliferation of pancreatic cancer cells in a paracrine manner, we silenced *Smo* mRNA expression in these cancer cells using small interfering RNA (Fig. 5c, left panels). Proliferation of *Smo*-silenced cancer cells decreased compared with that of wild-type cancer cells (data not shown). LPS-stimulated THP-1 cells enhanced the proliferation of control siRNA transfected cancer cells. However, when *Smo*-silenced cancer cells were used as target cells, this enhanced proliferation by LPS-stimulated THP-1 cells was significantly suppressed (Fig. 5c, right panels).

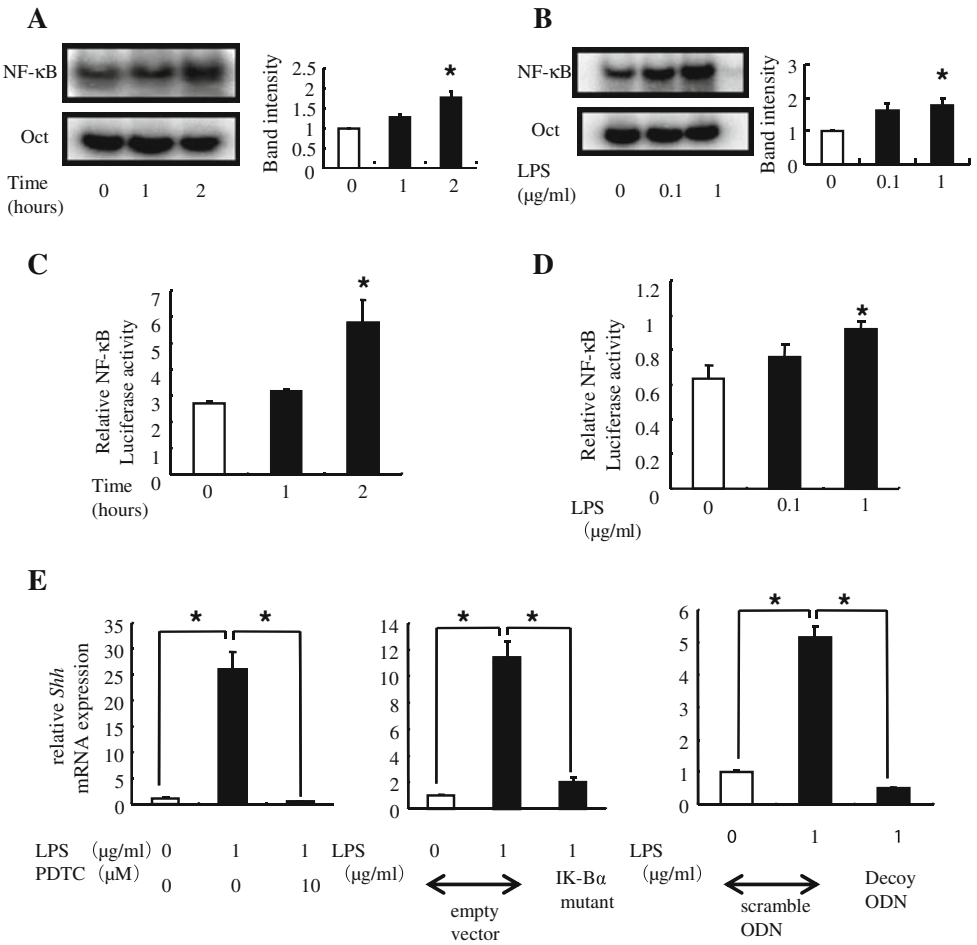

Fig. 3 LPS induces NF-κB activation in THP-1 cells and NF-κB inhibitor suppresses LPS-induced *Shh* mRNA expression. **a** THP-1 cells were treated with 1 μg/ml LPS for the indicated times and NF-κB binding activities were examined by EMSA (*left panel*). Band intensities were normalized (*right panel*). **b** THP-1 cells were treated with LPS at the indicated concentrations for 4 h and NF-κB binding activities were estimated by EMSA (*left panel*). Band intensities were normalized (*right panel*). **c** THP-1 cells were treated with 1 μg/ml LPS at the indicated times and NF-κB transcriptional activity was evaluated by luciferase assay. Relative NF-κB luciferase activity, normalized to *Renilla* luciferase activity. **d** THP-1 cells were treated with LPS at the indicated concentrations for 4 h and NF-κB transcriptional activity was evaluated by luciferase assay. **e** NF-κB inhibitors suppress NF-κB activation in THP-1 cells. *Left* Cells were treated with 10 μM PDTC for 24 h, and were treated with 1 μg/ml LPS for 24 h. *Shh* mRNA expression was evaluated by real-time PCR. *Center* Cells were co-transfected with empty vector or IκBα mutant and reporter plasmids for 48 h, and were treated with 1 μg/ml LPS for 24 h. *Shh* mRNA expression was evaluated by real-time PCR. *Right* Cells were co-transfected with scramble or NF-κB decoy ODN for 48 h, and were treated with 1 μg/ml LPS for 24 h. *Shh* mRNA expression was evaluated by real-time PCR. *Bars* SD. $^*P < 0.05$

Macrophages in PDAC specimens express Shh

Finally, we examined if Shh is produced at tumor sites, especially in macrophages. When tumor tissues were doubly stained with fluorescence-labeled antibodies against Shh (green) and CD68 (red) which is specifically expressed on macrophages and monocytes, double positive cells (yellow) were clearly detected in 9 of the 20 PDAC specimens examined. A representative case, in which numerous Shh-producing macrophages infiltrate into tumor site (dotted line), was shown (Fig. 6a). In this case, tumor cells also produce Shh. Our findings are simply summarized in Fig. 6b. Briefly, LPS induces Shh production in monocytes at tumor sites through NF-κB activation. Shh produced by monocytes increases the proliferation of PDAC cells through Hh pathway activation in a paracrine manner. Of course, Shh produced by pancreatic cancer cells themselves also increases the proliferation of PDAC in an autocrine manner.

Discussion

In the present study, we have indicated that inflammatory tumor-infiltrating monocytes (TAMs), probably macrophages, play an important role in the progression of PDAC

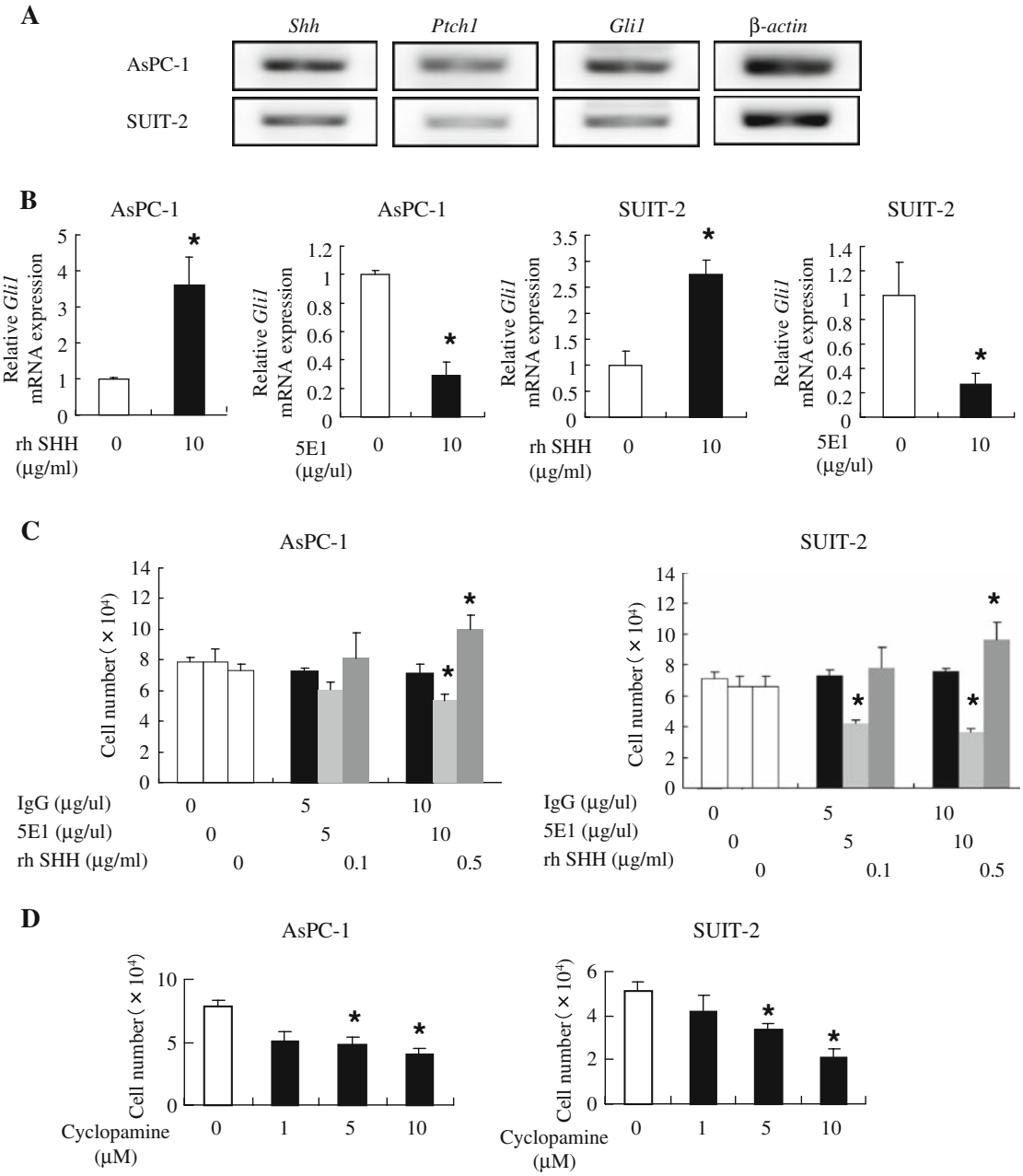

Fig. 4 Pancreatic cancer cells express Hh pathway-related molecules. **a** mRNA expressions of *Shh*, *Ptch1* and *Gli1* in AsPC-1 and SUIT-2 cells were examined by RT-PCR. *β-actin* was used for control. **b** When recombinant Shh (rh SHH) was added, *Gli1* mRNA expression significantly increased. In contrast, anti-SHH antibody (5E1) was added, *Gli1* mRNA expression significantly suppressed. **c** Cells were treated with recombinant human Shh at the indicated concentrations for 3 days and total cell number was counted with a Coulter counter. Cells were treated with 5E1 anti-Shh antibody at the indicated concentrations for 3 days and total cell number was counted with a Coulter counter. **d** Cells were treated with cyclopamine at the indicated concentrations for 3 days and total cell number was counted with a Coulter counter. *Bars* SD. $*P < 0.05$

cells through Shh production at the tumor site. Several studies, including ours, have indicated that Shh produced by tumor cells contributes in an autocrine manner to carcinogenesis and the progression of PDAC [25, 27, 35]. In fact, the Hh pathway is constitutively activated in two human pancreatic cancer cell lines used here because Gli1, which is a marker of the Hh pathway [10, 13, 31], was constitutively expressed in these cell lines. In addition, an antibody against Shh decreases Gli1 expression and proliferation of these cells in in vitro culture systems. Our present study demonstrated that silencing of Shh expression decreased the proliferation of these cells. Collectively, these data strongly indicate a contribution of autocrine Shh signaling to proliferation of these cells.

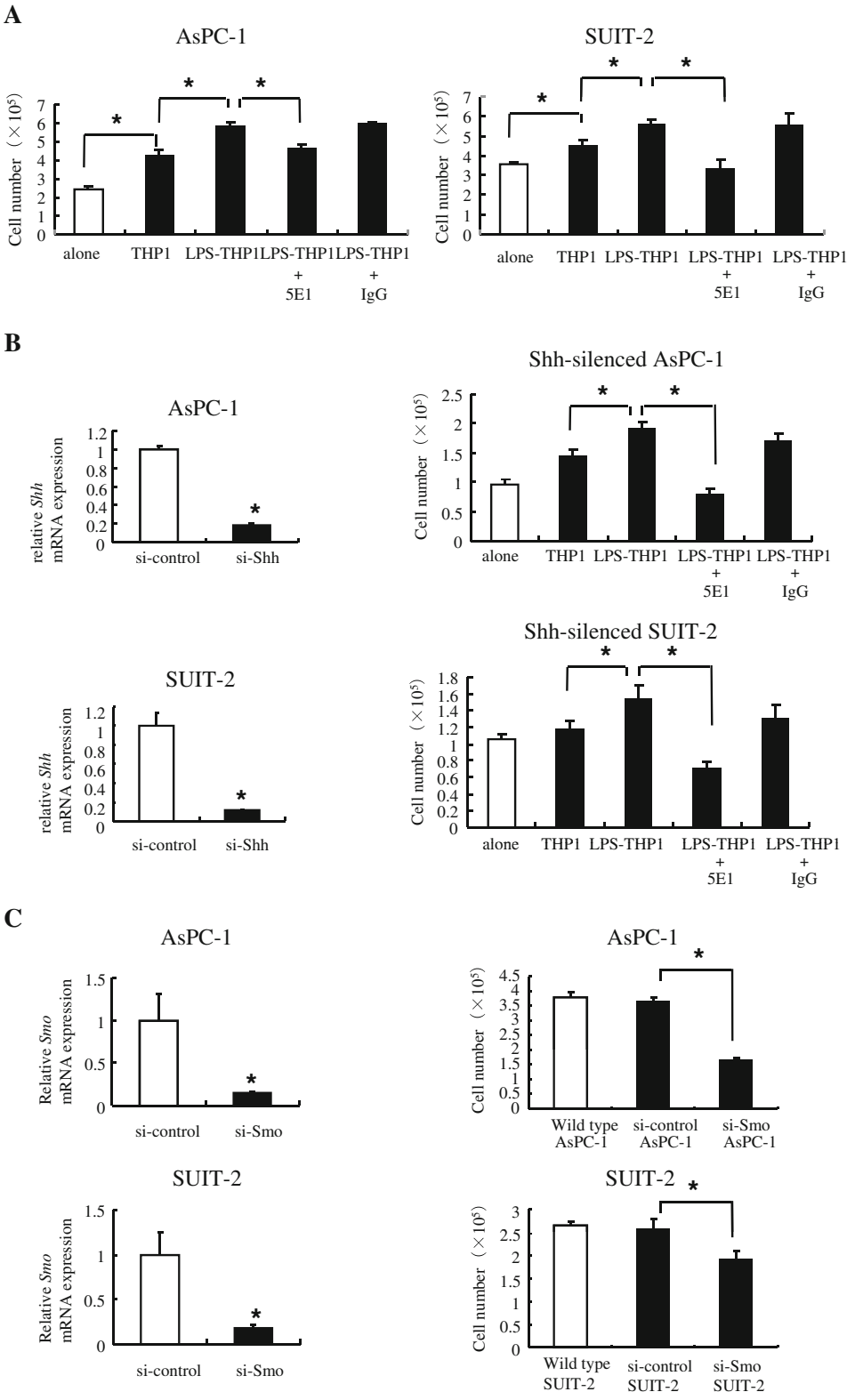

Fig. 5 Shh produced by LPS-stimulated THP-1 cells promotes proliferation of pancreatic cancer cells A, THP-1 cells were cultured in the presence or absence of LPS for 24 h. THP-1 cells were then washed intensively to eliminate LPS and the cell number was readjusted. AsPC-1 or SUIT-2 was cocultured with non-stimulated THP-1 cells, LPS-stimulated THP-1 cells or LPS-stimulated THP-1 cells with 5E1 or IgG antibody for 4 days. Total cell number was counted with a Coulter counter. The fractions of THP-1 cells and PDAC cells were determined using a FACSCalibur™ and the absolute number of PDAC cells was calculated. **b** AsPC-1 or SUIT-2 was transfected with siRNA for Shh or control siRNA by Lipofectamine for 36 h, and the expression of *Shh* mRNA was evaluated by real-time PCR (*left panels*). Shh-silenced AsPC-1 or SUIT-2 was cocultured with non-stimulated THP-1 cells, LPS-stimulated THP-1 cells, or LPS-stimulated THP-1 cells with 5E1 or IgG antibody for 4 days. Total cell number was counted with a Coulter counter. The fractions of THP-1 cells and PDAC cells were determined using a FACSCalibur™ and the absolute number of PDAC cells was calculated. *Bars* SD.* $P < 0.05$. **c** AsPC-1 or SUIT-2 was transfected with siRNA for Smo or control siRNA by Lipofectamine for 36 h, and the expression of *Smo* mRNA was evaluated by real-time PCR (*left panels*). Wild-type, control siRNA or Smo-siRNA transfected AsPC-1 or SUIT-2 was cocultured with LPS-stimulated THP-1 cells for 4 days. Total cell number was counted with a Coulter counter. The fractions of THP-1 cells and PDAC cells were determined using a FACSCalibur™ and the absolute number of PDAC cells was calculated. *Bars* SD. *$P < 0.05$

We have also shown for the first time a possible linkage between Shh expression and NF-κB activation in these PDAC cells [25]. Importantly, a recent paper showed that Shh is a direct transcriptional target of NF-κB [17]. Since tumor tissues consist of tumor cells and stromal cells, there is a possibility that NF-κB-activated stromal cells produces Shh and increases proliferation of PDAC cells in a paracrine manner. A relationship between chronic inflammation,

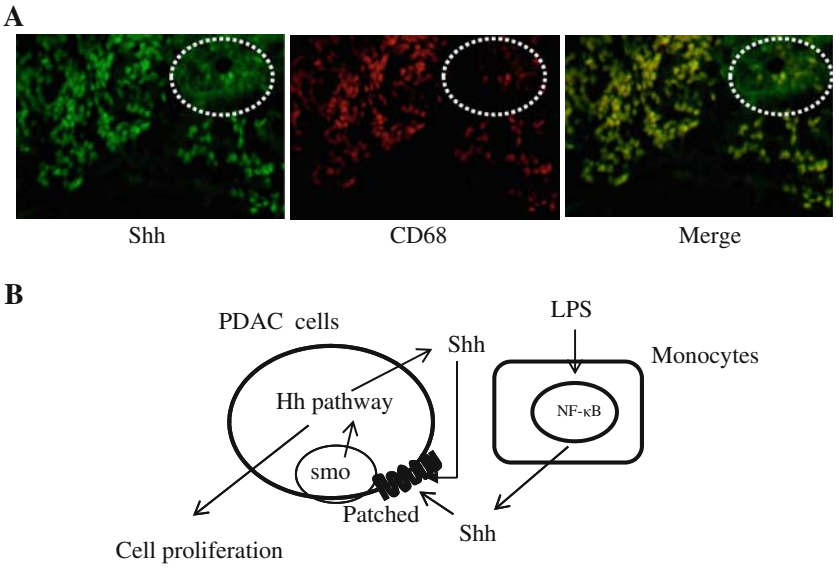

Fig. 6 Macrophages in PDAC specimens produce Shh. **a** Tumor tissues were doubly stained with fluorescence-labeled antibodies against Shh (*green*; *left picture*) and CD68 (*red*; *middle picture*). In this representative case, numerous Shh-producing macrophages (*yellow*; *right picture*) were found. Tumor cells also produce Shh (*dotted line*). **b** Schematic figure of our findings. LPS induces Shh production in monocytes through NF-κB activation. Shh produced by monocytes also increases the proliferation of PDAC cells through Hh pathway activation in a paracrine manner

carcinogenesis and progression of PDAC has long been supposed [10, 13, 31]. In addition, several investigators have indicated TAMs as the main cells linking chronic inflammation and the progression of PDAC [29]. In the present study, therefore, we used LPS and THP-1 cells as a NF-κB activator and target cells. As we expected, LPS increased Shh production in human monocytes and THP-1 cells through NF-κB activation and that LPS-stimulated THP-1 cells increased PDAC cell proliferation. We know that LPS can also increase Shh production through NF-κB activation in PDAC cells [25]. To minimize the contamination of LPS in our culture system, THP-1 cells were extensively washed before coculture with PDAC cells. To confirm that Shh produced by LPS-stimulated THP-1 cells, but not PDAC cells, can increase proliferation of PDAC cells, Shh-silenced PDAC cells were used as target cells because the PDAC cells used here produce Shh spontaneously. LPS-stimulated THP-1 cells also increased the proliferation of Shh-silenced PDAC cells and this increased proliferation was suppressed by a Shh antibody. These findings strongly indicate that Shh produced by LPS-stimulated THP-1 cells can increase PDAC cell proliferation in a paracrine manner.

Recently, a paracrine paradigm for Hh pathway-mediated carcinogenesis in PDAC has been the focus of various studies [36, 38]. Briefly, de Sauvage's group indicated that PDAC cells secrete Hh ligands, including Shh, to induce tumor-promoting Hh target genes in the adjacent stroma. Importantly, they also indicated that the pancreatic epithelium is not receptive of tumor cell-derived Hh ligands, but instead, Hh ligands promote PDAC via a paracrine signaling mechanism received by tumor stromal cells. In fact, NF-κB activation in TAMs induces production of several tumor-promoting proteins and plays important roles in carcinogenesis and progression of PDAC [29]. Thus, it still remains a possibility that THP-1-producing Shh activates the Hh pathway of THP-1 cells themselves in an autocrine manner, inducing the production of PDAC cell-proliferating molecules, and consequently increases indirectly PDAC cell proliferation. However, which molecules are induced in LPS-stimulated THP-1 cells by Hh pathway activation is as yet unknown. If such a paracrine mechanism functions in vivo, our data propose that NF-κB-activated monocytes may be one of the Shh supplying cells in addition to PDAC cells and play a significant direct and/or indirect roles in progression of PDAC, including proliferation, invasion and metastasis [12, 24].

In conclusion, our present study suggests that Hh pathway inhibitors may be a valid therapeutic or preventive strategy for PDAC, because these can inhibit Hh pathway activation in both PDAC cells and stromal cells such as monocytes.

Acknowledgments This study was supported by General Scientific Research Grants (21390363) from the Ministry of Education, Culture, Sports and Technology of Japan. We thank Dr. K. Takeda for kindly providing us with the NF-κB-dependent luciferase reporter, Dr. Aubie Shaw for kindly providing us with pSHH-GFP plasmids, and Dr. H. Yamamoto from Department of Anatomic Pathology, Kyushu University, for giving us an appropriate technical advice about immunohistochemistry. We also thank Kaori Nomiyama for the skillful technical assistance.

References

1. Auwerx J (1991) The human leukemia cell line, THP-1: a multifaceted model for the study of monocyte–macrophage differentiation. Experientia 47(1):22–31
2. Bansal P, Sonnenberg A (1995) Pancreatitis is a risk factor for pancreatic cancer. Gastroenterology 109:247–251

3. Berman DM, Karhadkar SS, Maitra A, Montes De Oca R, Gerstenblith MR, Briggs K, Parker AR, Shimada Y, Eshleman JR, Watkins DN, Beachy PA (2003) Widespread requirement for Hedgehog ligand stimulation in growth of digestive tract tumours. Nature 425:846–851
4. Boyle P, Maisonneuve P, Bueno de Mesquita B, Ghadirian P, Howe GR, Zatonski W, Baghurst P, Moerman CJ, Simard A, Miller AB, Przewoniak K, McMichael AJ, Hsieh CC, Walker AM (1996) Cigarette smoking and pancreas cancer: a case–control study of the search programme of the IARC. Int J Cancer 67:63–71
5. Bumcrot DA, Takada R, McMahon AP (1995) Proteolytic processing yields two secreted forms of sonic hedgehog. Mol Cell Biol 15:2294–2303
6. Cassol E, Alfano M, Biswas P, Poli G (2006) Monocyte-derived macrophages and myeloid cell lines as targets of HIV-1 replication and persistence. J Leukoc Biol 80:1018–1030
7. Chomczynski P, Sacchi N (1987) Single-step method of RNA isolation by acid guanidinium thiocyanate–phenol–chloroform extraction. Anal Biochem 162:156–159
8. Crouse NR, Ajit D, Udan ML, Nichols MR (2009) Oligomeric amyloid-beta(1–42) induces THP-1 human monocyte adhesion and maturation. Brain Res 1254:109–119
9. de Visser KE, Eichten A, Coussens LM (2006) Paradoxical roles of the immune system during cancer development. Nat Rev Cancer 6:24–37
10. Dunaeva M, Michelson P, Kogerman P, Toftgard R (2003) Characterization of the physical interaction of Gli proteins with SUFU proteins. J Biol Chem 278:5116–5122
11. Fan L, Pepicelli CV, Dibble CC, Catbagan W, Zarycki JL, Laciak R, Gipp J, Shaw A, Lamm ML, Munoz A, Lipinski R, Thrasher JB, Bushman W (2004) Hedgehog signaling promotes prostate xenograft tumor growth. Endocrinology 145:3961–3970
12. Feldmann G, Dhara S, Fendrich V, Bedja D, Beaty R, Mullendore M, Karikari C, Alvarez H, Iacobuzio-Donahue C, Jimeno A, Gabrielson KL, Matsui W, Maitra A (2007) Blockade of hedgehog signaling inhibits pancreatic cancer invasion and metastases: a new paradigm for combination therapy in solid cancers. Cancer Res 67:2187–2196
13. Ingham PW, McMahon AP (2001) Hedgehog signaling in animal development: paradigms and principles. Genes Dev 15:3059–3087
14. Izzi V, Chiurchiù V, D'Aquilio F, Palumbo C, Tresoldi I, Modesti A, Baldini MP (2009) Differential effects of malignant mesothelioma cells on THP-1 monocytes and macrophages. Int J Oncol 34:543–550
15. Karin M, Greten FR (2005) NF-kappaB: linking inflammation and immunity to cancer development and progression. Nat Rev Immunol 5:749–759
16. Karin M (2006) Nuclear factor-kappaB in cancer development and progression. Nature 441:431–436
17. Kasperczyk H, Baumann B, Debatin KM, Fulda S (2009) Characterization of sonic hedgehog as a novel NF-kappaB target gene that promotes NF-kappaB-mediated apoptosis resistance and tumor growth in vivo. FASEB J 23:21–33
18. Kuga H, Morisaki T, Nakamura K, Onishi H, Noshiro H, Uchiyama A, Tanaka M, Katano M (2003) Interferon-gamma suppresses transforming growth factor-beta-induced invasion of gastric carcinoma cells through cross-talk of Smad pathway in a three-dimensional culture model. Oncogene 22:7838–7847
19. Kusano KF, Pola R, Murayama T, Curry C, Kawamoto A, Iwakura A, Shintani S, Ii M, Asai J, Tkebuchava T, Thorne T, Takenaka H, Aikawa R, Goukassian D, von Samson P, Hamada H, Yoon YS, Silver M, Eaton E, Ma H, Heyd L, Kearney M, Munger W, Porter JA, Kishore R, Losordo DW (2005) Sonic hedgehog myocardial gene therapy: tissue repair through transient reconstitution of embryonic signaling. Nat Med 11:1197–1204
20. Li Q, Withoff S, Verma IM (2005) Inflammation-associated cancer: NF-kappaB is the lynchpin. Trends Immunol 26:318–325
21. Lowenfels AB, Maisonneuve P, Cavallini G, Ammann RW, Lankisch PG, Andersen JR, Dimagno EP, Andren-Sandberg A, Domellof L (1993) Pancreatitis and the risk of pancreatic cancer. International Pancreatitis Study Group. N Engl J Med 328:1433–1437
22. Luo JL, Maeda S, Hsu LC, Yagita H, Karin M (2004) Inhibition of NF-kappaB in cancer cells converts inflammation-induced tumor growth mediated by TNFalpha to TRAIL-mediated tumor regression. Cancer Cell 6:297–305
23. Morton JP, Mongeau ME, Klimstra DS, Morris JP, Lee YC, Kawaguchi Y, Wright CV, Hebrok M, Lewis BC (2007) Sonic hedgehog acts at multiple stages during pancreatic tumorigenesis. Proc Natl Acad Sci USA 104:5103–5108
24. Nagai S, Nakamura M, Yanai K, Wada J, Akiyoshi T, Nakashima H, Ohuchida K, Sato N, Tanaka M, Katano M (2008) Gli1 contributes to the invasiveness of pancreatic cancer through matrix metalloproteinase-9 activation. Cancer Sci 99:1377–1384
25. Nakashima H, Nakamura M, Yamaguchi H, Yamanaka N, Akiyoshi T, Koga K, Yamaguchi K, Tsuneyoshi M, Tanaka M, Katano M (2006) Nuclear factor-kappaB contributes to hedgehog signaling pathway activation through sonic hedgehog induction in pancreatic cancer. Cancer Res 66:7041–7049
26. Otsuki M (2003) Chronic pancreatitis in Japan: epidemiology, prognosis, diagnostic criteria, and future problems. J Gastroenterol 38:315–326
27. Pasca di Magliano M, Sekine S, Ermilov A, Ferris J, Dlugosz AA, Hebrok M (2006) Hedgehog/Ras interactions regulate early stages of pancreatic cancer. Genes Dev 20:3161–3173
28. Preiss S, Namgaladze D, Brüne B (2007) Critical role for classical PKC in activating Akt by phospholipase A2-modified LDL in monocytic cells. Cardiovasc Res 73:833–840
29. Pollard JW (2004) Tumour-educated macrophages promote tumour progression and metastasis. Nat Rev Cancer 4:71–78
30. Raderer M, Kurtaran A, Yang Q, Meghdadi S, Vorbeck F, Hejna M, Angelberger P, Kornek G, Pidlich J, Scheithauer W, Virgolini I (1998) Iodine-123-vasoactive intestinal peptide receptor scanning in patients with pancreatic cancer. J Nucl Med 39:1570–1575
31. Sasaki H, Nishizaki Y, Hui C, Nakafuku M, Kondoh H (1999) Regulation of Gli2 and Gli3 activities by an amino-terminal repression domain: implication of Gli2 and Gli3 as primary mediators of Shh signaling. Development 126:3915–3924
32. Sato S, Sugiyama M, Yamamoto M, Watanabe Y, Kawai T, Takeda K, Akira S (2003) Toll/IL-1 receptor domain-containing adaptor inducing IFN-beta (TRIF) associates with TNF receptor-associated factor 6 and TANK-binding kinase 1, and activates two distinct transcription factors, NF-kappa B and IFN-regulatory factor-3, in the Toll-like receptor signaling. J Immunol 171:4304–4310
33. Schnoor M, Buers I, Sietmann A, Brodde MF, Hofnagel O, Robenek H, Lorkowski S (2009) Efficient non-viral transfection of THP-1 cells. J Immunol Methods 344:109–115
34. Schreck R, Schreck R, Meier B, Männel DN, Dröge W, Baeuerle PA (1992) Dithiocarbamates as potent inhibitors of nuclear factor kappa B activation in intact cells. J Exp Med 175:1181–1194
35. Thayer SP, di Magliano MP, Heiser PW, Nielsen CM, Roberts DJ, Lauwers GY, Qi YP, Gysin S, Fernandez-del Castillo C, Yajnik V, Antoniu B, McMahon M, Warshaw AL, Hebrok M (2003) Hedgehog is an early and late mediator of pancreatic cancer tumorigenesis. Nature 425:851–856
36. Tian H, Callahan CA, DuPree KJ, Darbonne WC, Ahn CP, Scales SJ, de Sauvage FJ (2009) Hedgehog signaling is restricted to the stromal compartment during pancreatic carcinogenesis. Proc Natl Acad Sci USA 106:4254–4259

37. Yamanaka N, Morisaki T, Nakashima H, Tasaki A, Kubo M, Kuga H, Nakahara C, Nakamura K, Noshiro H, Yao T, Tsuneyoshi M, Tanaka M, Katano M (2004) Interleukin 1beta enhances invasive ability of gastric carcinoma through nuclear factor-kappaB activation. Clin Cancer Res 10:1853–1859
38. Yauch RL, Gould SE, Scales SJ, Tang T, Tian H, Ahn CP, Marshall D, Fu L, Januario T, Kallop D, Nannini-Pepe M, Kotkow K, Marsters JC, Rubin LL, de Sauvage FJ (2008) A paracrine requirement for hedgehog signalling in cancer. Nature 455:406–410
39. Zhang B, Ma Y, Guo H, Sun B, Niu R, Ying G, Zhang N (2009) Akt2 is required for macrophage chemotaxis. Eur J Immunol 39:894–901